Advances in Cement Research, 2005, **17**, No. 3, July, 121–132

Experimental study and modelling of heat evolution of blended cements

K. A. Paine*, L. Zheng* and R. K. Dhir*

University of Dundee

The advisability of controlling the temperature rise and fall in concrete at early age is well recognised, and the choice of an appropriate, low-heat cement with suitable heat of hydration characteristics can assist in this control. This is particularly pertinent with respect to water-retaining and massive concrete structures where the need to prevent early-age thermal cracking is paramount. Portland cement/ground granulated blast furnace slag (PC/ggbs) or PC/fly ash cements are often used in these structures due to their low heat hydration properties. This paper presents the results of isothermal conduction calorimetry tests carried out on PC/ggbs and PC/fly ash cements and describes a model that uses these results to simulate the heat evolution processes in hydration concrete sections at early ages. The tests covered a range up to 90% ggbs and up to 65% fly ash content by mass of cement, at temperatures from 5° to 60°C. For PC/ggbs cements, the total heat of hydration can be considered as a composition of three components, that is heats from an initial Portland cement reaction, a latent ggbs hydraulic reaction and co-reactivity effects of PC and ggbs; whereas for PC/fly ash cements, the initial PC reaction dominated with a small co-reactivity effect.

Introduction

The advisability of controlling the temperature rise and fall in concrete at early age is well recognised as one of the major factors in preventing early-age thermal cracking.[1,2] When concrete is externally restrained and the difference between the peak temperature inside the concrete core and mean ambient is large, temperature gradients across the concrete section can initiate visual cracking. If these cracks are not minimised and crack widths controlled, cracking may seriously affect serviceability. As a result the need to prevent early-age thermal cracking is paramount with respect to water-retaining and massive concrete structures. The degree of temperature loss in concrete can be controlled by various means and the use of low heat cement is effective.[3,4] Indeed, blended cements consisting of Portland cement (PC) and ground granulated blast furnace slag (ggbs) or fly ash are widely used throughout the world, because they have low heat of hydration while producing concrete with excellent long-term strength and durability, as a result of latent hydraulic or pozzolanic reactions.[1,4–6]

In order to simulate the heat evolution inside a concrete structure and predict the peak temperature, it is vital to establish a proper hydration model of the cement. Currently, cement hydration models play an important role in prediction of the temperature distribution inside concrete, and are used to predict concrete formwork striking times[7] and simulate microstructure formation and degradation processes.[8–11] A number of cement hydration models have been published.[5,8–14] However, from the view of concrete temperature simulation, some models are over-complicated, requiring a large number of parameters, many of which are not available in general engineering practice; for example cement mineral compositions, such as C_3S, C_2S, C_3A and C_4AF content, and their particle sizes. On the other hand, some models are over-simplified and cannot be used to vary non-PC content in cement combinations. Thus, they cannot be used to proportion blended cement combinations in order to optimise temperature control and concrete performance.

This paper describes an experimental and theoretical study carried out to develop a hydration model for PC/ggbs and PC/fly ash blended cements to estimate the early-age temperature of concrete structures. It enables the effect of blended cement composition to be taken into account, and makes it possible to predict an

* Concrete Technology Unit, Division of Civil Engineering, University of Dundee, Dundee, Scotland, DD1 4HN.

(ACR 4488) Paper received 22 April 2004; last revised 22 March 2005; accepted 22 March 2005.

optimum cement combination for controlling concrete performance.

Experimental programme

In this study, a systematic series of isothermal conduction calorimetry tests for PC/ggbs and PC/fly ash blended cements were carried out at temperatures of 5, 20, 40 and 60°C, and the effect of cement composition on the heat evolution performance examined. The curves of rate of heat evolution against time and cumulative heat were analysed and a mathematical model based on the test results proposed.

Materials

A single Portland cement, strength class 42·5N conforming to BS EN 197-1[15] was used throughout. Two sources of ggbs, denoted GA and GB, and two sources of fly ash, FA and FB, were used to prepare different blended cements. The physical and chemical properties are shown in Table 1. Additions GA and FA were finer than GB and FB, respectively.

Cement combinations and test programme

To examine the effect of ggbs and fly ash content on the heat of hydration, isothermal calorimetry tests were carried out over a range of combination contents including 100% PC, four different ggbs contents, 35, 50, 70 and 90% by mass, and three fly ash contents, 35, 50, and 65% by mass. For each test, 30 g cement was used and the water/cement ratio (w/c) was fixed at 0·5. To ascertain the 'apparent activation energy', each cement combination was tested at four different temperatures: 5, 20, 40 and 60°C.

The isothermal conduction calorimeter used was a JAF conduction calorimeter manufactured by Wexham Developments, UK. The heat evolution process up to 72 h was recorded and calculated using software supplied by the manufacturer.

Experimental results

Portland cement

Table 2 gives: (*a*) the time to attain the maximum rate of heat evolution; (*b*) maximum heat evolution, W/kg; (*c*) total heat up to the maximum rate of heat evolution; and (*d*) cumulative heat at 72 h, for PC at 5, 20, 40 and 60°C.

The rate of heat evolution, q, against time, t, and cumulative heat, Q_{cc}, are shown in Fig. 1. The rate is characterised by smooth curves and a clear maximum rate of heat evolution. The maximum rate of heat

Table 1. Properties of cements and additions used in study

Property	PC	GGBS		Fly ash	
		GA	GB	FA	FB
Relative density	3·14	2·86	2·88	2·14	2·06
Fineness: m^2/kg	405	602	466	7·2†	35·0†
Particle size distribution: % passing by volume					
125 μm	100	100	100	100	97·3
100 μm	100	100	99·9	99·8	93·0
75 μm	99·8	100	99·6	97·7	85·9
45 μm	96·6	98·7	96·6	88·7	69·9
25 μm	81·8	91·2	84·9	70·9	50·7
10 μm	41·2	62·4	53·7	41·6	28·5
5 μm	19·7	41·5	34·5	24·6	16·9
2 μm	7·7	21·4	17·1	10·9	7·7
1 μm	4·3	10·5	8·1	5·5	3·8
0·7 μm	2·4	5·5	4·1	3·0	2·0
0·5 μm	0·8	1·7	1·3	1·0	0·6
0·2 μm	0·1	0·2	0·1	0·1	0·1
Bulk oxide composition					
SiO_2	21·5	35·2	36·3	44·2	46·6
Al_2O_3	5·4	13·1	12·6	29·0	29·3
Fe_2O_3	2·6	0·2	0·5	5·9	6·5
CaO	64·2	41·0	42·1	2·2	2·2
MgO	2·6	8·1	6·9	0·9	0·8
P_2O_5	0·1	0·0	0·0	0·6	0·5
TiO_2	0·3	0·7	0·6	1·5	1·4
SO_3	2·8	1·3	1·1	0·6	0·7
K_2O	0·7	0·5	0·3	1·2	1·1
Na_2O	0·3	0·2	0·2	0·2	0·2
MnO	0·0	0·5	0·3	0·0	0·0

† % by mass retained on 45μm sieve.

Table 2. Results of isothermal conduction calorimetry tests for PC

Test temperature °C	Time to max. rate of heat evolution, t_{max}: h	Max. rate of heat evolution, q_{max}, W/kg	Heat output at q_{max}, Q_{tm}: kJ/kg	Heat output at 72 h, Q_{t72}: kJ/kg
5	21·5	1·24	55·8	189·1
20	8·90	3·30	59·1	266·1
40	3·80	9·16	53·9	305·9
60	1·21	22·0	56·0	347·5

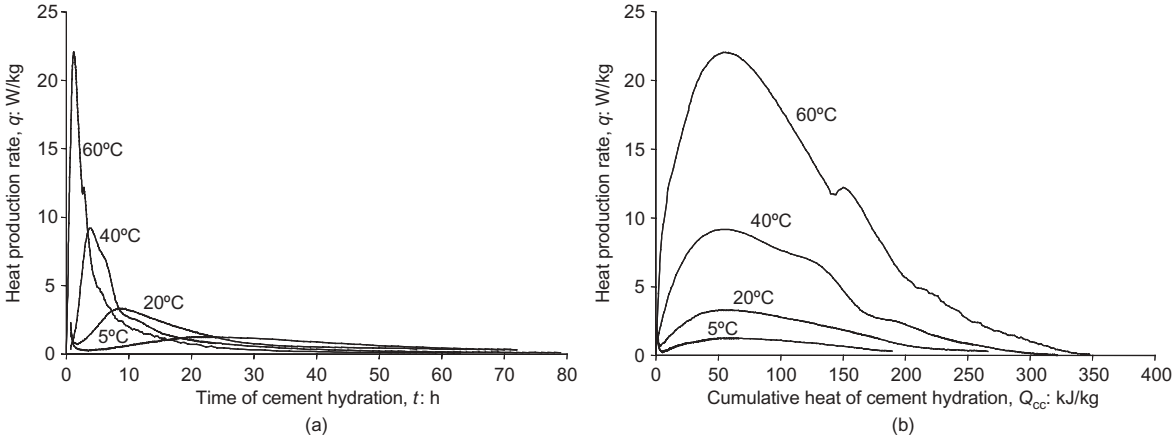

Fig. 1. Rate of heat evolution of Portland cement, (a) q against t and (b) q against Q_{cc}

evolution, q_{max}, increases with an increase in hydration temperature and the time to reach the maximum rate of heat evolution is shorter at higher temperatures (Fig. 1(a)).

In Fig. 1(b), it can be seen that the cumulative heat, Q_{tm}, at q_{max} is similar for different hydration temperatures, and ranges from 50 to 60 kJ/kg, for the PC tested over the temperature range from 5 to 60°C. This is similar to the results of De Schutter,[5,16] in which the measured temperature range was 5 to 35°C. The importance of this plot of heat evolution rate against cumulative heat is that although no fundamental relation exists, Q_{cc} reflects the relative degree of hydration of the solids; moreover, an approximate constant for the activation energy, E, of PC hydration can be derived.

The measured cumulative heat at 72 h hydration was greater for the higher temperatures. This was anticipated since, in a given time, the higher the temperature, the higher the degree of hydration of the cement.

PC/ggbs cements

Typical curves of the rate of heat evolution, q, against time, t, and cumulative heat, Q_{cc}, for PC/ggbs cements are shown in Figs 2 and 3. In general, the relationships are characterised by double maxima, which are considered to result from an initial Portland cement reaction, followed by a later ggbs reaction

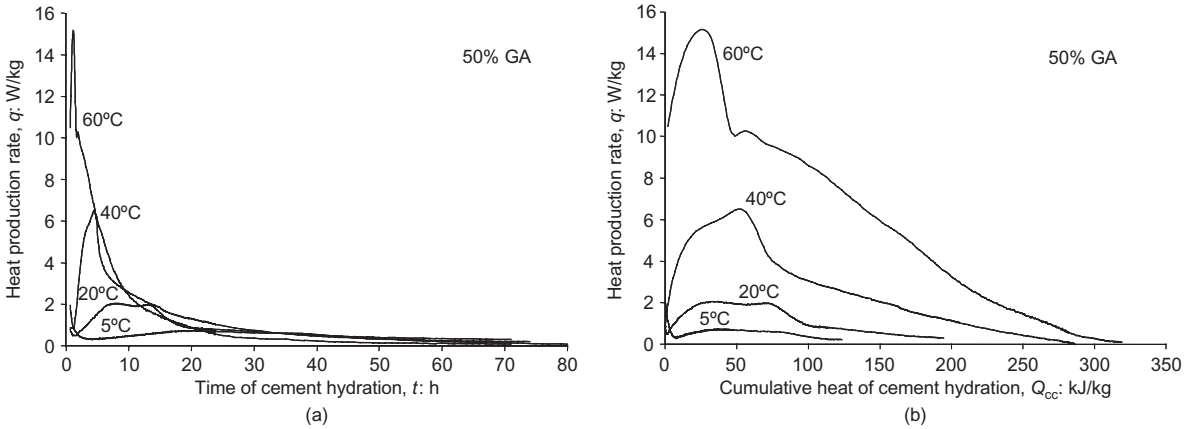

Fig. 2. Rate of heat evolution of 50%PC/50%GA cement combination, (a) q against t and (b) q against Q_{cc}

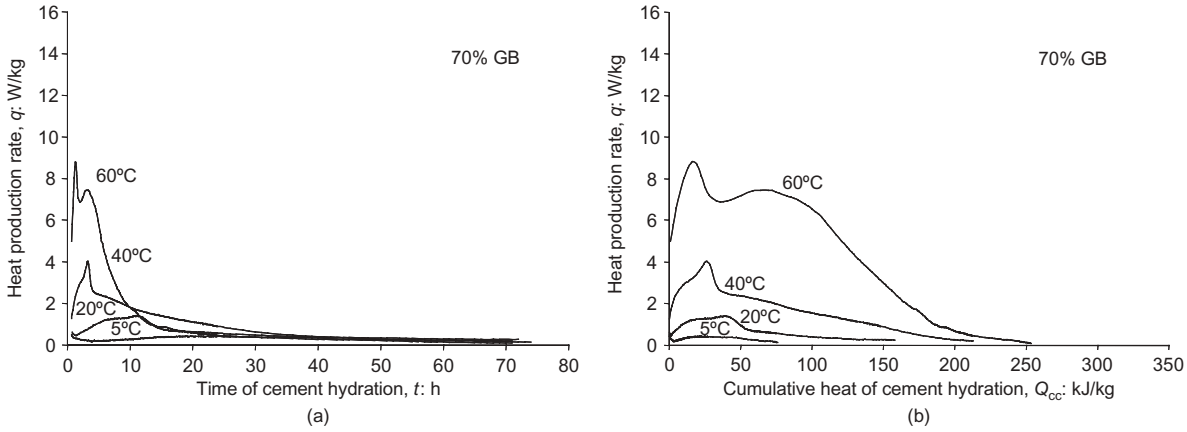

Fig. 3. Rate of heat evolution of 30%PC/70%GB cement combination, (a) q against t and (b) q against Q_{cc}

activated by the portlandite liberated by hydration of the Portland cement. However, the second peak tended to become coincident with the first peak at 60°C.

The heat evolution curves were similar for the two types of ggbs, when comparing the same temperature. The rate of heat evolution and total heat output for GA was greater than that of GB, reflecting the higher fineness and greater reactivity of GA. Comparisons of the curves of rate of heat evolution against cumulative heat are shown in Fig. 4; the difference in heat evolution rates between GA and GB becomes more apparent at higher hydration temperatures.

The effects of ggbs content on the maximum rate of heat evolution are shown in Fig. 5. An approximately linear relationship between the two parameters is observed for both types of PC/ggbs cement combinations over the range of measurements.

The relationships between cumulative heat at 72 h and ggbs content are shown in Fig. 6. Nearly linear relationships are obtained at the lower temperatures, 5–20°C, with the relationship becoming less linear at higher temperatures, 40–60°C. From the figure, it can be seen that ggbs cement with less than 50% ggbs can generate more heat than PC at high temperatures, especially when GA, the more reactive ggbs, was used. This phenomenon has also been reported by other researchers.[17,18] However, for higher ggbs content blends, say ggbs contents greater than 70%, this phenomenon will not occur.

PC/fly ash cements

Some typical curves of the rate of heat evolution, q, against time, t, and cumulative heat, Q_{cc}, for PC/fly ash cements are shown in Figs 7 and 8, respectively. Generally, the relationships show a small tendency towards two maxima but these are clearly less defined that those of ggbs cements, and the second maximum is generally lower than the first maximum which is attributed to hydration of the Portland cement.

Comparisons of rate of heat evolution against cumulative heat of the two types of fly ash cements are shown in Fig. 9. The two fly ash cements gave similar curves for the same temperature. The rate of heat evolution and cumulative heat for FA was marginally greater than that of FB, reflecting the greater fineness of FA.

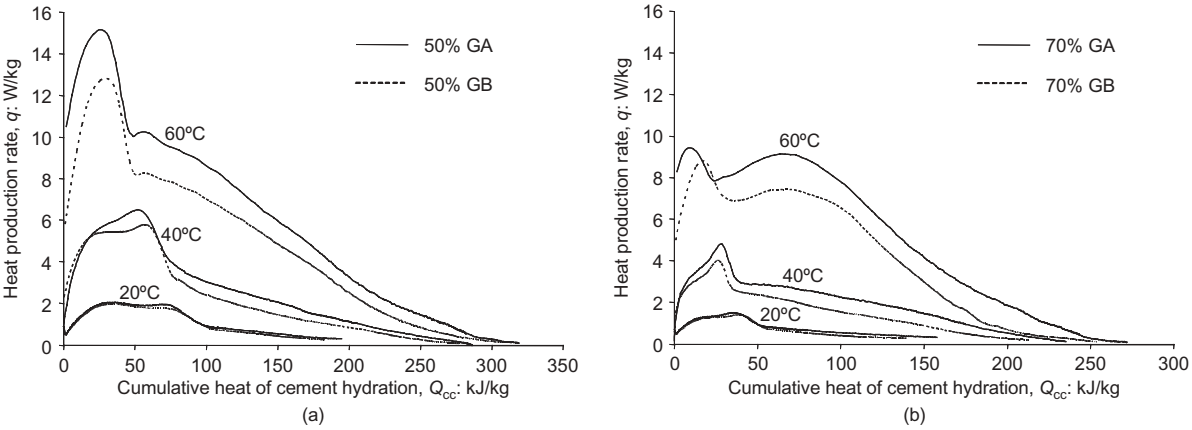

Fig. 4. Comparison of q against Q_{cc} curves between the two PC/ggbs cement combinations, (a) 50% ggbs cement and (b) 70% ggbs cement

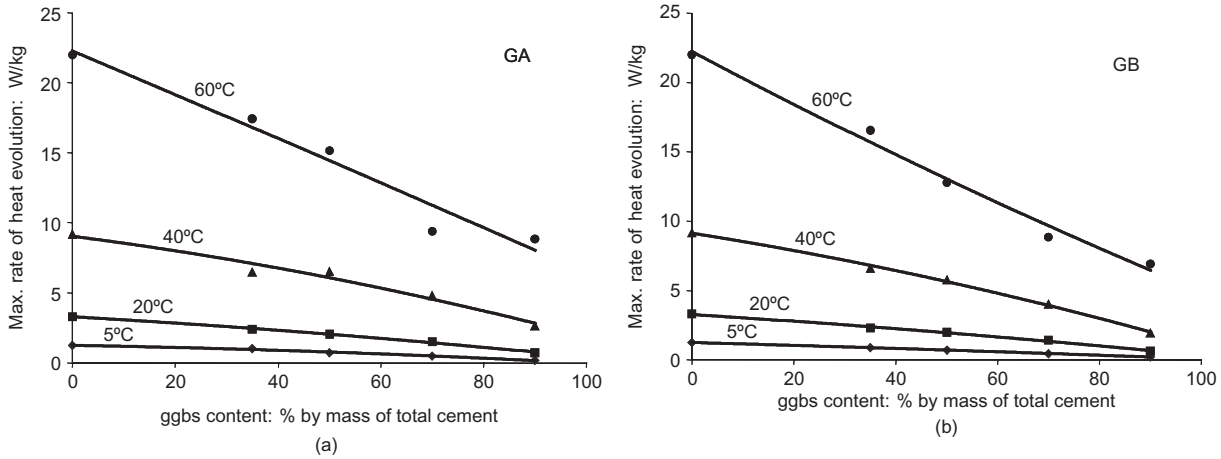

Fig. 5. Relationship between maximum rate of heat evolution and ggbs content, (a) PC/GA cement combination and (b) PC/GB cement combination

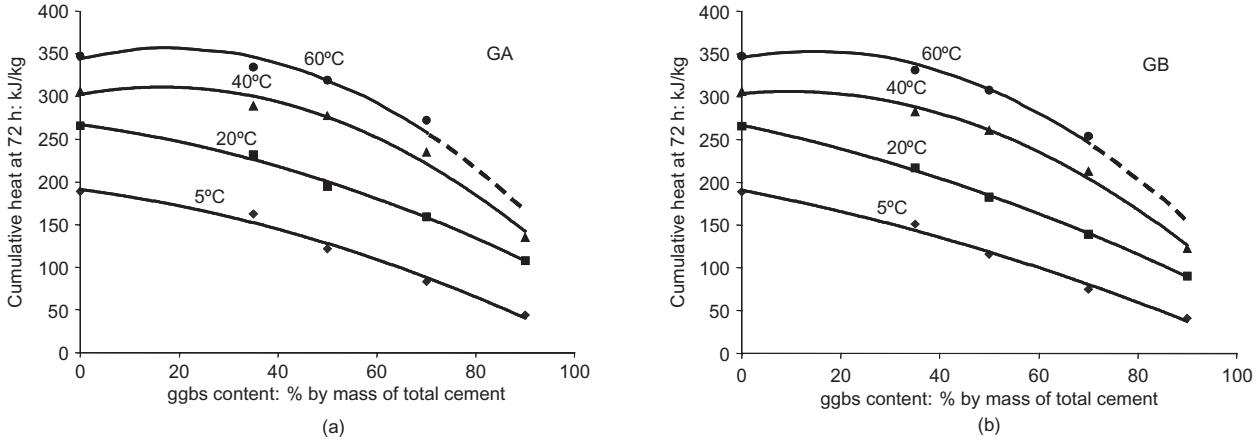

Fig. 6. Relationship between total heat after 72 h and ggbs content, (a) PC/GA cement combination and (b) PC/GB cement combination

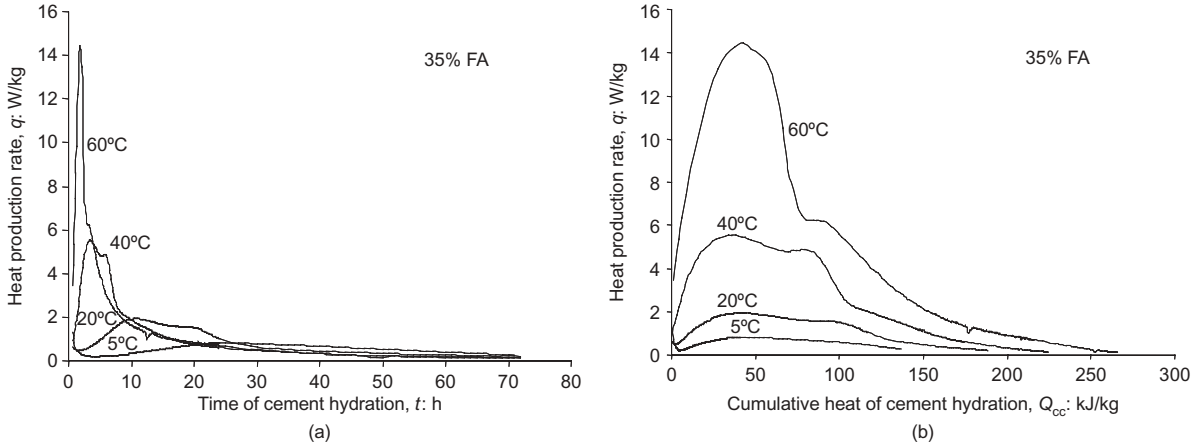

Fig. 7. Rate of heat evolution of 65%PC/35%FA cement combination, (a) q against t and (b) q against Q_{cc}

The effect of fly ash content on the maximum rate of heat evolution is shown in Fig. 10, and as with the ggbs cements, a linear relationship exists between the two parameters. However, the differences between the results of the two fly ash cements were negligible. This would be expected because the highest rate is due to PC reaction, and is not generally influenced by fly ash. Linear relationships were found between cumulative heat at 72 h and fly ash contents (Fig. 11). However, the linear relationships exist even at higher temperatures, showing that the pozzolanic reaction of fly ash has little influence on the total heat generated up to

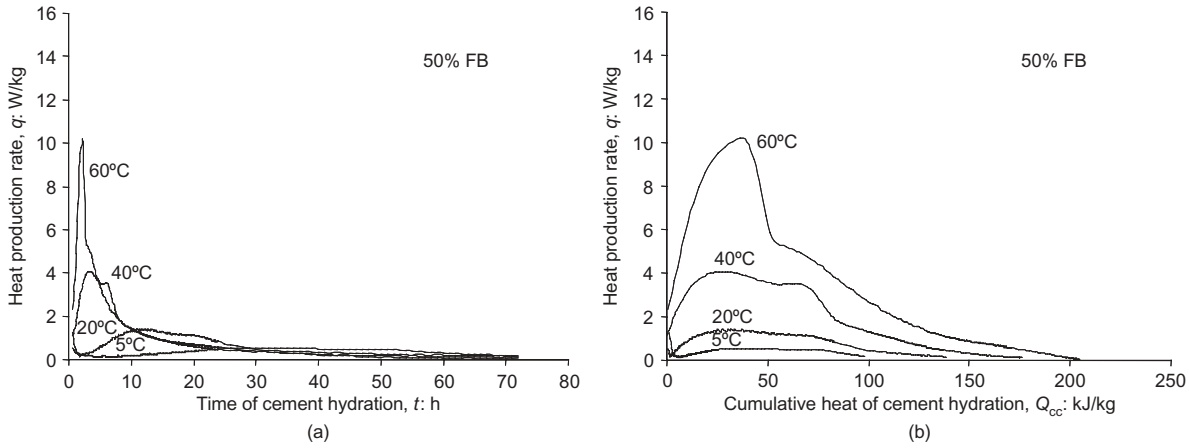

Fig. 8. Rate of heat evolution of 50%PC/50%FB cement combination, (a) q against t and (b) q against Q_{cc}

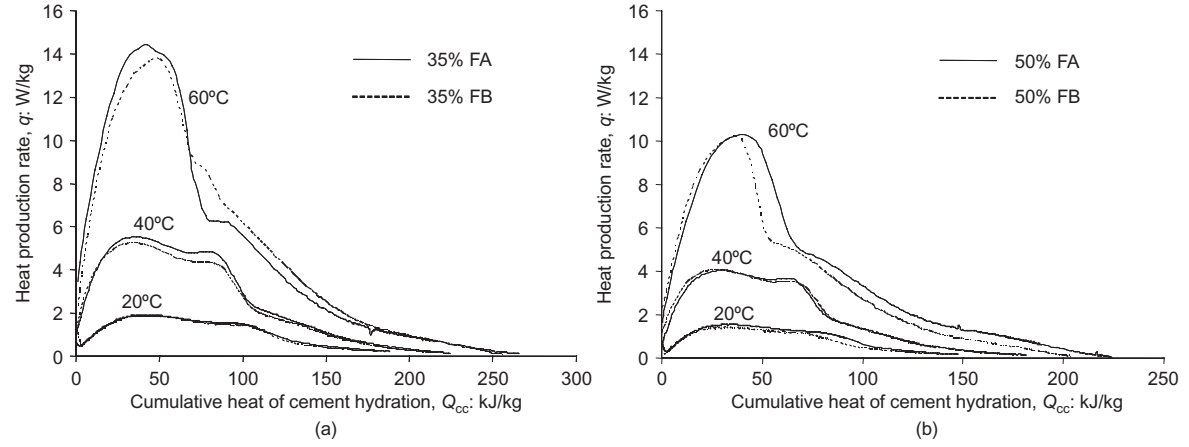

Fig. 9. Comparison of q against Q_{cc} curves between the two PC/fly ash cement combinations, (a) 35% fly ash cement and (b) 50% fly ash cement

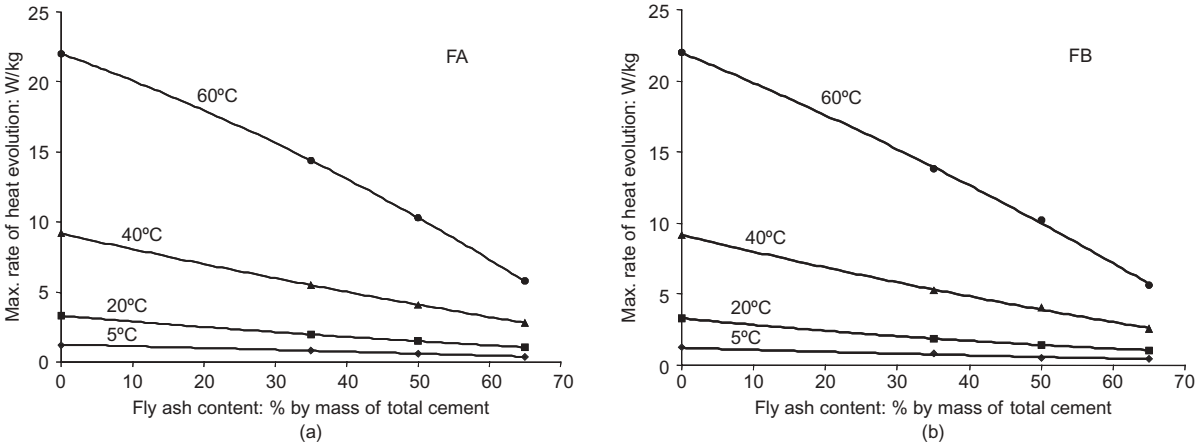

Fig. 10. Relationship between maximum rate of heat evolution and fly ash content, (a) PC/FA cement combination and (b) PC/FB cement combination

72 h (the time frame in which the temperature peaks, and therefore the maximum thermal gradient in concrete will be achieved). Beyond 72 h, it is likely that the pozzolanic reaction will have an increasingly significant effect on total heat.

Hydration modelling

Portland cement

Examination of several cement hydration models and comparison with the results obtained in this study found that the De Schutter model[5,16] was accurate in

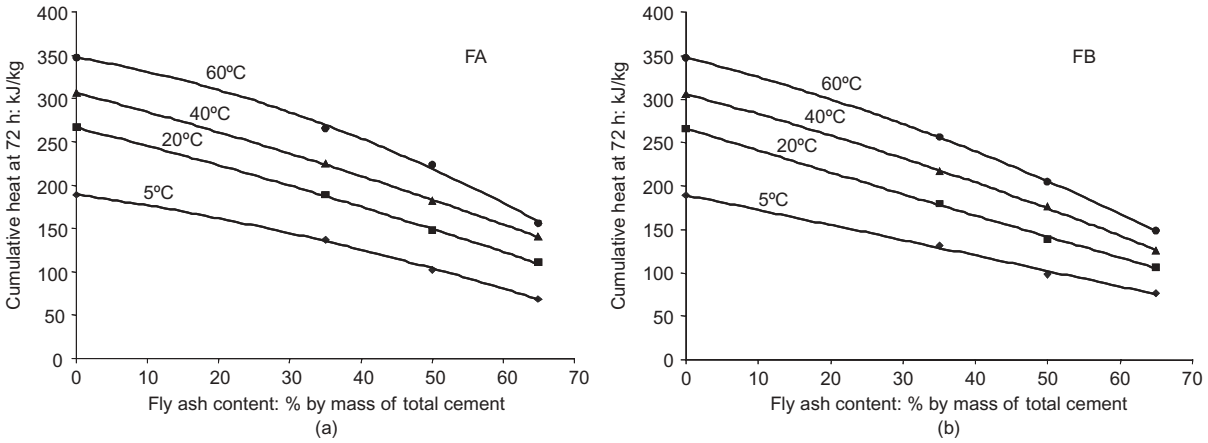

Fig. 11. Relationship between total heat after 72 hours and fly ash content, (a) PC/FA cement combination and (b) PC/FB cement combination

describing the hydration of Portland cement. The relationship between rate of hydration heat and degree of hydration at 20°C for PC proposed by De Schutter is given as follows

$$q_{20} = q_{\max 20} f(r)$$
$$f(r) = c[\sin(r\pi)]^a \exp(-br) \quad (1)$$
$$r = Q_{cc}(t)/Q_{\max}$$

where $q_{\max 20}$ is the maximum heat hydration rate of PC at 20°C; $Q_{cc}(t)$ is the cumulative heat of hydration at t; $Q_{\max}$ is the total heat of hydration released at the end of the reaction; and a, b, c are constants.

In considering the effect of temperature on the hydration, the Arrhenius function has been chosen; when heat is produced by a zero-order chemical reaction, the rate of heat production may be represented by the following function[19]

$$q = q_0 \times \exp\left[\frac{-E(Q_{cc})}{R(273+T)}\right] \quad (2)$$

where q_0, k are constants and $E(Q_{cc})$ is the apparent activation energy at Q_{cc}. It is approximately a constant for PC hydration and simply expressed as E hereafter.

R is the universal gas constant, and when $T_{ref} = 20$°C (293 K) and q_{20} are used as a reference

$$q = q_{20} \times \exp\left[\frac{E}{R}\left(\frac{1}{293} - \frac{1}{273+T}\right)\right] \quad (3)$$

Based on the test data, parameters in the formulae above can be calibrated as given in Table 3 together with De Schutter's original model parameters. The differences between the two sets of parameters reflect the different hydration characteristics of the cements used in this study and by De Schutter. The curves from the model simulation and the measured data are shown in Fig. 12.

Table 3. Modelling parameters for PC hydration

	Modelling parameters for PC hydration	
	(calibrated by the data from this study)	(De Schutter's original published parameters)
a	0·875	0·667
b	5·0	3·0
c	4·22	2·60
$q_{\max 20}$: W/kg	3·30	2·16
$Q_{\max}$: kJ/kg	350·0	270·0
E: kJ/mol	38·5	33·5

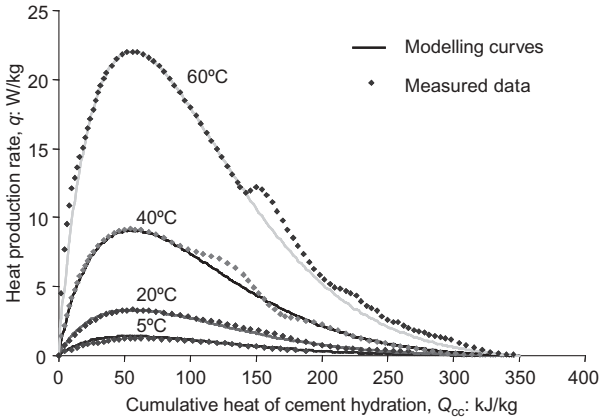

Fig. 12. Model curves and test data for PC

PC/ggbs cements

Although De Schutter has proposed a model for ggbs cement hydration,[5,16] this model does not relate the heat production rate to the ggbs content. Indeed, when the model was applied to the results obtained in this study, no meaningful relationships were found between the model parameters and ggbs content. Therefore, a refined model was required to deal with this variable. Based on the experimental work, the following model has been proposed.

(*a*) Heat production rate, q, of the cement hydration was divided into three portions: (*i*) a PC hydration, q_p; (*ii*) a ggbs hydration, q_s and (*iii*) a co-reactivity effect of PC and additions, q_r, namely

$$q = q_p + q_s + q_r \quad (4)$$

Similar model patterns to equation (1) and (3) were used for both PC and ggbs hydrations:

$$q_{p,20} = q_{p,max20} f_p(r)$$
$$f_p(r) = c_p[\sin(r\pi)]^{a_p} \exp(-b_p r) \quad (5)$$

and

$$q_{s,20} = q_{s,max20} f_s(r)$$
$$f_s(r) = c_s[\sin(r\pi)]^{a_s} \exp(-b_s r) \quad (6)$$

where $q_{p,max20}$ is the maximum heat hydration rate of PC at 20°C; $q_{s,max20}$ is the maximum heat hydration rate of ggbs at 20°C; r is $Q_{cc}(t)/Q_{max}$; $Q_{cc}(t)$ is the cumulated heat of hydration at t; Q_{max} is the total heat of hydration released at the end of the reaction; a_p, b_p, c_p are constants for PC hydration; and a_s, b_s, c_s are constants for ggbs hydration.

The Arrhenius functions are expressed as

$$q_p = q_{p20} \times \exp\left[\frac{E_p}{R}\left(\frac{1}{293} - \frac{1}{273+T}\right)\right] \quad (7)$$

and

$$q_s = q_{s20} \times \exp\left[\frac{E_s}{R}\left(\frac{1}{293} - \frac{1}{273+T}\right)\right] \quad (8)$$

where E_p is the apparent activation energy for PC and E_s is the apparent activation energy for ggbs.

It is assumed that both E_p and E_s are constants that are only associated with the chemical reactivity of PC and ggbs respectively, and are independent of PC/ggbs proportions. For a given ggbs content in cement, the modelling process is divided into three steps as illustrated schematically in Fig. 13. Take 70% GB cement as an example.

Step 1. Modelling PC hydration q_p. Test results of the 70% GB cement at temperatures 5, 20, 40 and 60°C are shown in Fig. 13(a), an adapted version of Fig. 3(b). Based on the PC modelling results given in Table 3 and Fig. 12, it can be shown that

$$q_{p,max20} = (100 - GB\%)/100 \times q_{max20}$$
$$= (100 - 70)/100 \times 3{\cdot}30 = 0{\cdot}99(W/kg)$$
$$E_p = E = 38{\cdot}5\ (kJ/mol)$$

The total Q_{max} can be obtained by extending the q–Q_{cc} curves to the point $q = 0$. In this example,

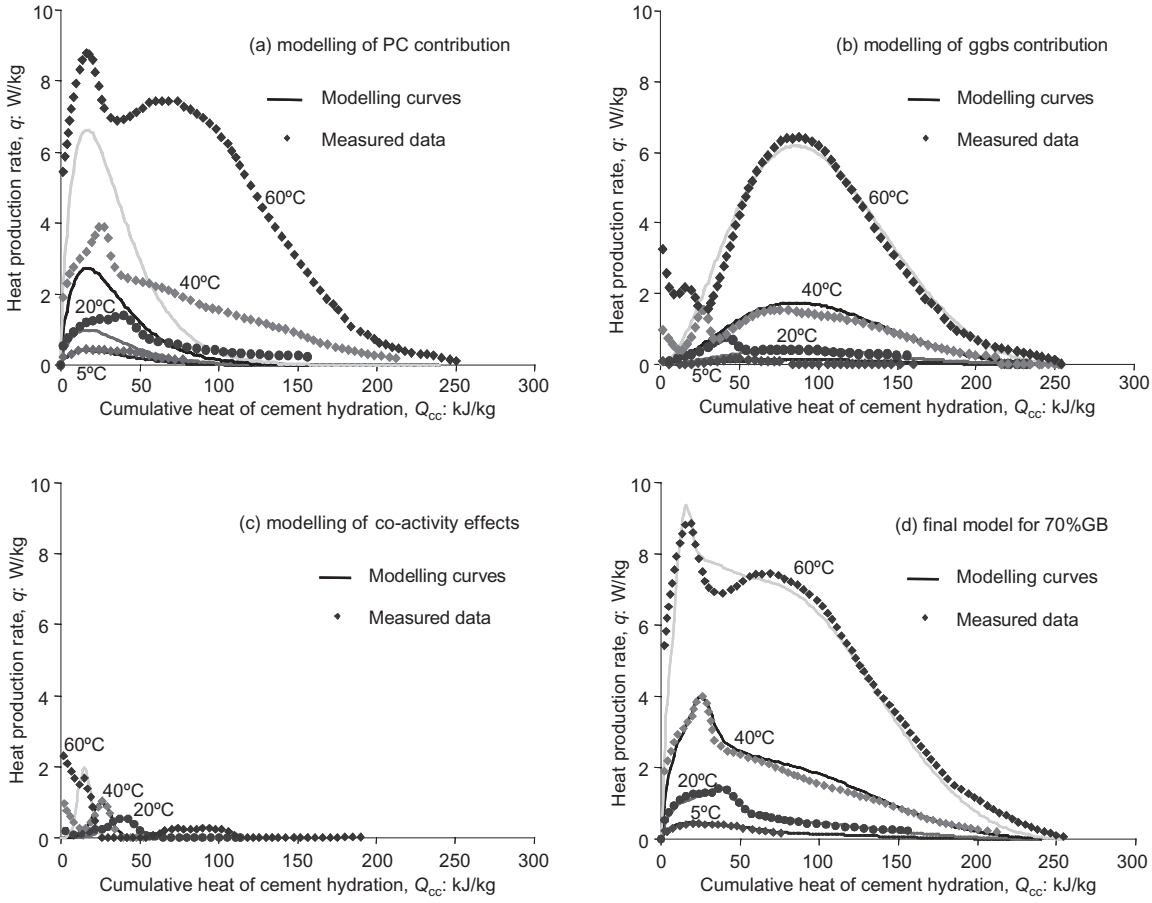

Fig. 13. Modelling process for ggbs cement

$Q_{max} = 255$ kJ/kg as shown in Fig. 13(a). When inconsistency was found from different curve extensions, the value was taken according to the curves measured at higher temperature since the extended section was short and the error can be ignored.

Of the three constants a_p, b_p and c_p, a_p is fixed at 0·875 as obtained in Table 3, b_p is derived such that the time to maximum rate of heat evolution is the same as that of plain PC and c_p is adjusted so that $f_p(r) = 1$ at the point $q_{p,20} = q_{p,max20}$. The modelling curves of the PC contribution are also shown in Fig. 13(a).

Step 2. Modelling ggbs hydration q_s. Subtraction of the modelling q_p values from the total measured values gives the curves that result from ggbs hydration and the co-reactivity effect of PC and additions, as shown in Fig. 13(b). In Fig. 13(b), it can be seen that the main maximum, which occurs at $Q_{cc} = 86$ kJ/kg results from ggbs hydration, and modelling curves from equations (6) and (8) can be obtained as shown in Fig. 13(b). The modelling constants are

$$q_{s,max20} = 0{\cdot}41 \text{ (W/kg)}$$

$$E_s = 55{\cdot}0 \text{ (kJ/mol)}$$

Comparing the ggbs modelling curves with that of PC, it can be seen that PC hydration maxima occurred before the ggbs hydration maxima and that the E_s value is larger than E_p value. This agrees with the hydration characteristics of ggbs cement described in CIRIA Report 91[1] and by other researchers.[17,18]

Step 3. Modelling co-reactivity effects of PC and additions, q_r. After subtracting the modelling q_p and q_s values from the total results values, there is a residual heat which is unaccounted for. However, these small peaks are marginal as shown in Fig. 13(c), and no particular relationship can be found for them. These small peaks cannot belong to PC hydration or to ggbs hydration alone, but could result from some co-reactivity effects of PC clinker and additions, although further confirmation is required. (Note that here additions mean ggbs, fly ash or some other mineral materials blended into PC.). This remaining contribution can for practical purposes be ignored and only a small difference was found in the concrete temperature rise calculation. When judged by the area under the curves, the remaining part accounts for 5%, on average, of the total area.

It was thought that the co-reactivity effect could be caused by a number of independent small factors, some of which are mentioned in the literature,[17] for example, hydration of some components in the PC or ggbs being accelerated or delayed under particular solution and temperature conditions. In practice, their synthesis effect can be simulated by a normal distribution curve, expressed as the following equation.

$$q_r = a_r \exp\left[-\frac{(Q_{cc} - b_r)^2}{c_r}\right] \tag{9}$$

where a_r, b_r and c_r are constants for co-reactivity effects of PC and additions, and are dependent on temperature and the PC/ggbs combination.

Of the three constants, a_r determined the height of the peak, b_r determined its position and c_r determined its width. The modelling curves for these small peaks are also shown in Fig. 13(c). Fig. 13(d) shows the final modelling curves in comparison with the measured data.

By this method, hydration models for different PC/ggbs combinations can be derived. Fig. 14 shows some curves calculated from the model alongside the measured data for ggbs cements on which it was based. Table 4 gives values of all parameters for PC/GB combinations.

The relationships between $q_{p,max20}$ and $q_{s,max20}$ and ggbs contents are shown in Fig. 15. For PC hydration, the relationship was assumed linear. After subtracting

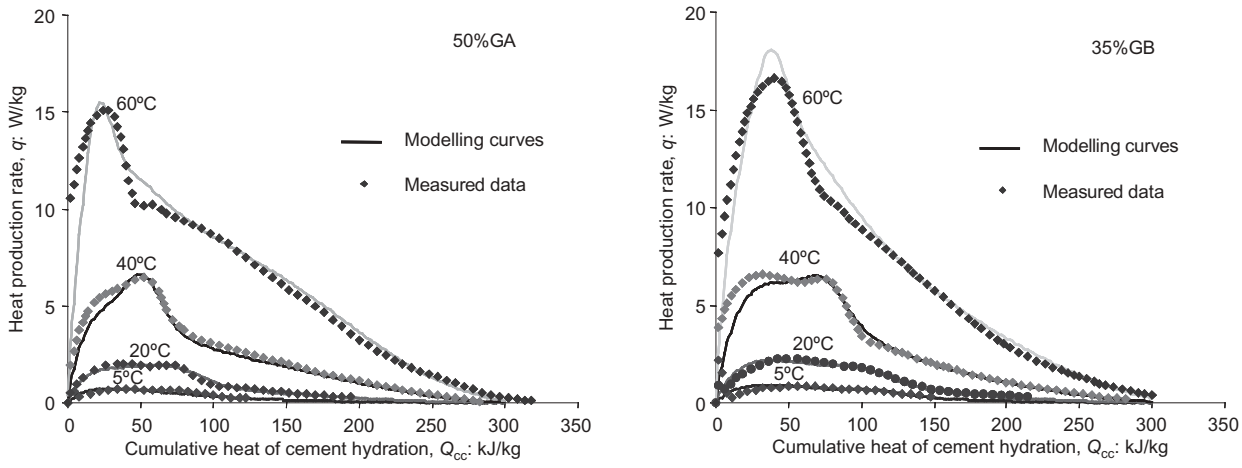

Fig. 14. Model curves and test data for ggbs cements, (a) 50%PC/50%GA cement combination and (b) 65%PC/35%GB cement combination

Table 4. Modelling parameters for PC/GB cement combinations

		Modelling parameters for PC/GB cement combination			
		35% GB	50% GB	70% GB	90% GB
Q_{max}: kJ/kg		335	310	255	200
a_p		0·875	0·875	0·875	0·875
b_p		7·738	9·425	13·355	31·169
c_p		6·040	7·137	9·634	20·145
$q_{p,max20}$: W/kg		2·15	1·65	0·99	0·33
E_p: kJ/mol		38·5	38·5	38·5	38·5
a_s		2·0	2·0	2·0	2·0
b_s		1·0	1·74	3·67	13·35
c_s		1·608	2·213	4·531	35·764
$q_{s,max20}$: W/kg		0·205	0·293	0·410	0·415
E_s: kJ/mol		55·0	55·0	55·0	55·0
a_r	5°C	0·222	0·133	0·065	0·080
	20°C	0·474	0·595	0·316	0·155
	40°C	0·621	0·698	0·452	0·198
	60°C	0·894	0·699	0·596	0·466
b_r	5°C	110	80	48	100
	20°C	100	76	36	97
	40°C	75	60	23	68
	60°C	38	30	15	10
c_r	5°C	648	450	450	5000
	20°C	800	578	200	4050
	40°C	392	288	98	1152
	60°C	200	32	72	72

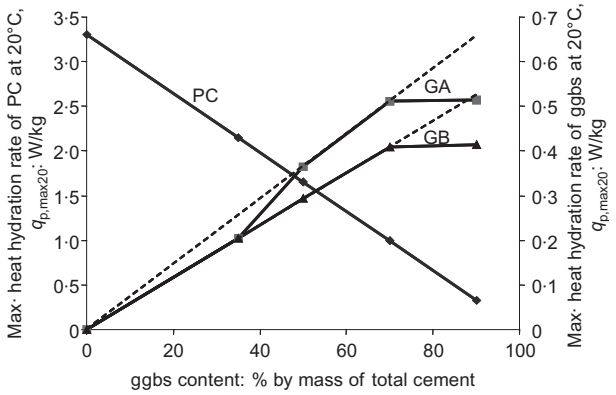

Fig. 15. Relationships of $q_{p,max20}$ and $q_{s,max20}$ to ggbs content

the modelling q_p values, the maximum heat of hydration rate for ggbs, $q_{s,max20}$, was found to be increasing linearly. However, since the hydration of ggbs requires portlandite made available during the PC hydration, this linear relationship only exists in a certain range, in which the release of $Ca(OH)_2$ matches the requirement for ggbs reaction. The results show that for ggbs contents greater than 70%, the potential $q_{s,max20}$ cannot be achieved due to the lack of $Ca(OH)_2$. As a result, there is a $q_{s,max20}$ plateau.

As the PC reaction and ggbs reaction occurred coincidently and co-reactivity effects in the PC/ggbs combination system existed, division of the total heat of hydration into heat from PC and ggbs, as used in De Schutter's original model, was not necessary in the model proposed.

PC/fly ash cements

A similar modelling process to that described for PC/ggbs cements above can be applied to modelling PC/fly ash cements. During fly ash cement hydration, fly ash initially accelerates the reaction of the Portland cement (co-reactivity effect) followed by pozzolanic reactions.[1] Unlike ggbs cements, the pozzolanic reactions of fly ash are small at early ages, and are therefore not significantly observed within the first 72 h of hydration. For this reason, the second reaction contribution, q_s, can be ignored in the modelling process. As a result, the heat production rate for fly ash cements, up to 72 h can be given as

$$Q = q_p + q_r \quad (10)$$

Figure 16 shows curves resulting from the model alongside the measured data for fly ash cements on which it was based. For predictions of temperature at later ages, q_s, the pozzolanic reaction, will need to be taken into account.

Conclusions and discussion

Systematic isothermal conduction calorimetry tests for PC/ggbs and PC/fly ash blended cements were

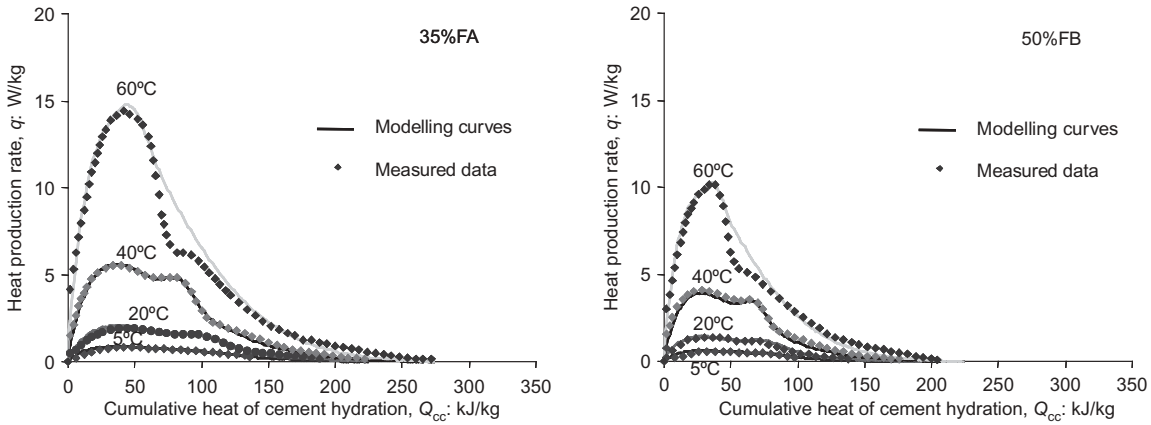

Fig. 16. Model curves and test data for fly ash cements, (a) 65%PC/35%FA cement combination and (b) 50%PC/50%FB cement combination

carried out for different cement combinations at different temperatures. Based on the experimental results, a mathematical model to simulate the hydration of blended cement is proposed. The model comprises three parts; an initial Portland cement reaction, co-reactivity effect of PC and additions, and a latent hydraulic/pozzolanic reaction. For fly ash the pozzolanic reaction was taken as zero at 72 h. De Schutter's PC hydration model was used to describe PC reaction. However, for the co-reactivity effect and ggbs reaction, a new model was developed. With this model, the effect of cement combinations can be taken into account and it is possible to design an optimum cement combination to achieve an optimal point for both temperature control and satisfactory concrete performance.

It should be recognised that the hydration process of blended cement is far more complex than a combination of three contributions as used in the model. The model presented in this paper reflects a balance of accuracy, complexity and information required. Following the modelling process provided in this study, a more accurate model can be established when for example cement mineral compositions, their individual hydration properties, and interactions are available. Whatever the complexity of a cement combination, it can be divided into n hydration components, in which each component obeys Arrhenius law and can be modelled using formulae in the form of equations (1)–(3), respectively. In addition, there exist several co-reactivity effects in the system, which do not obey Arrhenius law and they can be modelled using formulae in the form of equation (9). Further work is required to verify this inference.

A computer program using models described in this paper was developed to predict the temperature rise in concrete. Satisfactory predictions were obtained in relation to the several on-site concrete constructions. It was noted that the Wexham calorimeter used in the tests does not record early-age heat, yet this contributes to temperature rise. Computer simulation showed that the main effect of the early age heat is on the time to reach the peak temperature and has only a small effect on the peak temperature itself. Work is in progress to consider this effect as well as other effects, such as admixtures, affecting the temperature rise of the concrete.

Acknowledgements

The authors would like to acknowledge the support provided by the Department of Trade and Industry, Babtie Group, Castle Cement Ltd, Cementitious Slag Makers Association, Concrete Structures Group, John Doyle Construction Limited, Mott MacDonald, North of Scotland Water Authority, Quarry Products Association, Rugby Cement, and ScotAsh Ltd. Thanks are also given to Professor D. C. Spooner (formerly of the BCA) for supplying the prototype computer programs for concrete temperature simulation, and to Mr Oliver Hart for his assistance with the experimental work.

References

1. Harrison T. A. *Early-age Thermal Crack Control in Concrete*, Report 91. Construction Industry Research and Information Association, London, 1992.
2. Liu C., Meline R. and Lee J. N. Heat removal from mass concrete footing. *Concrete 2002 Transportation Research Record*, 2002, No. 1798, 39–42.
3. Furuya N. and Tatsumi M., Technical innovation for realization of Akashi-Kaikyo Bridge. *Proceedings of the Institution of Civil Engineers, Structures and Buildings*, 1994, **104**, No. 3, 285–296.
4. Tollow A. J. Durbans newest water-resource – the Inanda Dam. *Journal of the Institution of Water and Environmental Management*, 1991, **5**, No. 5, 519–528.
5. De Schutter G. Hydration and temperature development of concrete made with blast-furnace slag cement. *Cement and Concrete Research*, 1999, **29**, No. 1, 143–149.
6. Xiong X. and Van Breugel K. Apparent activation energy and its application in the numerical simulation of blended

cement hydration process. In *Challenges of Concrete Construction: Innovations and Developments in Concrete Materials and Construction*, (Dhir R. K., Hewlett P. C. and Csetenyi L. J. (eds)). Thomas Telford, London, 2002, pp. 91–100.
7. Harrison T. A. *Formwork Striking Times – Criteria, Prediction and Methods of Assessment*, Report 136. CIRIA, London, 1995.
8. Van Breugel K. HYMOSTRUC: A computer based simulation model for hydration and formation of structure in cement based materials. In *Hydration and Setting of Cements*, (Nonat A. and Mutin J. C. (eds)). RILEM, E & FN Spon, London, 1992, pp. 361–368.
9. Maekawa K., Chaube R. and Kishi T. *Modelling of Concrete Performance: Hydration, Microstructure Formation and Mass Transport*. E &FN Spon, London, 1999.
10. Bentz D. P. Three-dimensional computer simulation of Portland cement hydration and microstructure development. *Journal of the American Ceramic Society*, 1997, **80**, No. 1, 3–21.
11. Bentz D. P., Garboczi E. J. and Martys N. S. Application of digital-image-based models to microstructure, transport properties, and degradation of cement-based materials. In *The Modelling of Microstructure and Its Potential for Studying Transport Properties and Durability*. Kluwer Academic Publishers, Dordrecht, 1996, pp. 167–185.
12. Pitkänen P. Prediction of temperature fields of massive concrete structures during hardening. *Nordic Concrete Research*, 1984, **3**, 183–190.
13. Spooner D. C. BCA *Computer Model for Temperature Rise Prediction in Fresh Concrete*, British Cement Association, TDH 51062. CIRIA, London, 1992.
14. Wang C. and Dilger W. H. Prediction of temperature distribution in hardening concrete. In *Thermal Cracking in Concrete at Early Age*s, (Springenschmid R. (ed), *Proceedings of the International RILEM Symposium*, Institute of Building Materials, Technical University of Munich, Germany, E & FN Spon, London, 1994, pp. 21–28.
15. British Standards Institution. *BS EN 197-1:2000 Cement. Composition, Specifications and Conformity Criteria for Common Cements*. British Standards Institution, London, 2000.
16. De Schutter G. and Taerwe L. General hydration model for Portland cement and blast-furnace slag cement. *Cement and Concrete Research*, 1995, **25**, No. 3, 593–604.
17. Wu X., Roy D. M. and Langton C. A. Early stage hydration of slag cement. *Cement and Concrete Research*, 1983, **13**, No. 2, 227–286.
18. Uchikawa H. Effect of blending components on hydration and structures formation. *The Eighth International Congress on the Chemistry of Cement*, Rio, 1986, Vol. 1, pp. 249–280.
19. Carslaw H. S. and Jaeger J. C. *Conduction of Heat in Solids*, 2nd edition. Clarendon Press, Oxford, 1959, reprinted 1992.

Discussion contributions on this paper should reach the editor by 14 December 2005